Path specific Doppler compensation in time-reversal communications

Sérgio M. Jesus, Salman I. Siddiqui, and António Silva
Laboratory of Robotic Systems in Engineering and Science, Campus de Gambelas,
University of Algarve, 8005-139 Faro, Portugal
sjesus@ualg.pt, sijaz.23@gmail.com, asilva@ualg.pt

Abstract: Passive time reversal (pTR) is a low complexity receiver scheme that uses multichannel probing for time signal refocusing, thus reducing time spreading and improving inter-symbol interference. Recognizing that signals traveling through different paths are subject to arrival-angle-related Doppler displacements, this letter proposes a further improvement to pTR that applies correcting frequency shifts optimized for beams formed along each specific path arrival angle. The proposed channel equalizer is tested with real data, and the results show that the proposed approach outperforms both pTR and the modified pTR channel combiners providing an MSE gain of 4.9 and 4.2 dB, respectively.

1. Introduction

Reliable underwater acoustic coherent communications is still a great challenge due to environmental effects distorting the signal between emitter and receiver. Among the most impairing effects are channel multipath causing signal time spread and channel time-variability as well as source receiver relative motion causing Doppler spread. The standard approach is to design adaptive channel equalizers that attempt to compensate for the channel multipath and track ocean variability constantly minimizing its effect on the underwater communication system (see, e.g., Ref. 1, and references herein).

In the last decade, passive time reversal (pTR) also known as phase conjugation has emerged as an effective low-complexity channel multipath compensation technique.[2] In pTR communication, the signals received in an array of sensors are correlated with the time reversed versions of the estimated impulse responses (IR) of each channel, obtained at a previous time. This effectively recreates an ocean-replica based matched-filter at each sensor output that is then summed over all sensors to obtain spatial focusing and gain. Under optimal conditions of channel reciprocity, channel stability, and sufficient array physical span, the pTR output effectively deconvolves the channel from the transmitted signal, allowing for optimal detection and decoding of the transmitted message with low intersymbol interference (ISI) and reduced mean square error (MSE) Rouseff.[3] In Preisig,[4] the author compares the performance of the channel estimate-based decision feedback equalizer (DFE) and pTR in presence of imperfect channel estimates. The results suggest that the performance of pTR degrades significantly in the presence of rapid channel variations, e.g., sea surface waves and source-receiver motion. In addition to time spreading, the received signal also spreads in the frequency domain due to environmental variations (e.g., surface variations) and/ or geometric variations (e.g., source receiver relative motion).[5] These variations also affect the temporal focusing of the pTR communication system resulting in loss of performance. In Song *et al.*,[6] it was shown that a continuous channel update and Doppler tracking are required before pTR operation to achieve acceptable performance in presence of ocean variability.

In the multipath environment, the transmitted signal reaches the receiver through different paths where each path is affected by environmental variations in a

different manner, resulting in a different amount of Doppler in each path.[7] One way for dealing with these Doppler-multipath dispersions is to beamform the data and steer nulls in the direction of any other paths but the main arrival.[8] In current Doppler compensation techniques, Doppler distortion is compensated with a single value that fails to give maximum compensation.[9,10] In Silva *et al.*,[11] an improved version of pTR frequency shift pTR (FSpTR) was proposed that includes appropriate frequency shifts in the pTR impulse response estimates so as to maximize the output power at each time instant during the interval between successive probes. It was proved with both simulated and real data that FSpTR could provide an MSE gain of several decibels and in Vilaipornsawai *et al.*,[12] a DFE was integrated with FSpTR to improve the performance of the communication system. However, because each path is affected differently by environmental variations, FSpTR, which applies a single frequency shift correction for all the paths, fails to compensate accurately for channel variabilities resulting in residual ISI at the FSpTR system output. In this letter, a refinement of FSpTR is proposed where frequency shifts are adapted for each incoming wavefront separately, thus providing further compensation for path-specific environmental variations.

This letter is organized as follows: Sec. 2 will present the receiver structure using a delay-Doppler-based model. Section 3 will present comparative performance results obtained on real data. Section 4 concludes this letter.

2. Receiver structure

Delay-Doppler models are widely accepted for describing the transmission of narrowband signals over time-varying channels.[13] In such models, the lth sensor noiseless received complex baseband signal over a deterministic P-path channel is written as

$$r_l(t) = \sum_{p=1}^{P} h_p s(t - \alpha_{lp} - \tau_p) e^{j2\pi(t - \alpha_{lp})\nu_p}, \tag{1}$$

where $s(t)$ is the source transmitted signal, (h_p, τ_p, ν_p) are the complex amplitude, time delay, and Doppler shift characterizing path p, respectively, and α_{lp} is the array geometry dependent time delay for path p to reach sensor l. For a d-equispaced vertical line array (VLA) and assuming plane-wave propagation $\alpha_{lp} = (l - 1)d \cos \theta_p / c$, where θ_p is the arrival angle of path p and c is the sound speed. The simplification that consists in considering the parameters (h_p, τ_p, ν_p) sensor independent is justified by the sensor averaging of phase aligned fields after the conjugate multiplication (in the frequency domain) occurring in the time-reversal process (see Sec. 2.1). After sensor averaging, the path amplitudes are simply the average of signal magnitude squared over the array. Splitting the time delay of path p at sensor l as a delay τ_p and a plane-wave delay delay α_{lp} has the advantage of putting in evidence the beamform delay for applying the method proposed in Sec. 2.3. The narrow-band assumption generally implies that baseband bandpass transformation maybe represented by a simple frequency shift, which generally assumes a signal band $B \ll f_c$, where f_c is the carrier frequency. A frequency equivalent of Eq. (1) is given by

$$R_l(f) = \sum_{p=1}^{P} h_p a_l(\theta_p) S(f - \nu_p) e^{-j2\pi(f - \nu_p)\tau_p}, \tag{2}$$

where $a_l(\theta_p) = e^{-j2\pi f \alpha_{lp}}$, for the VLA case under the plane-wave assumption.

One channel of the pTR receiver structure is shown in the block diagram of Fig. 1. The signal $r'_l(t)$ is the received probe at true time $t = 0$, stored in memory and then reused to process the actual signal $r_l(t)$ received at true time $t > 0$. Gray shaded blocks allow for implementing the proposed variations of the basic pTR algorithm as described in Secs. 2.1 and 2.2.
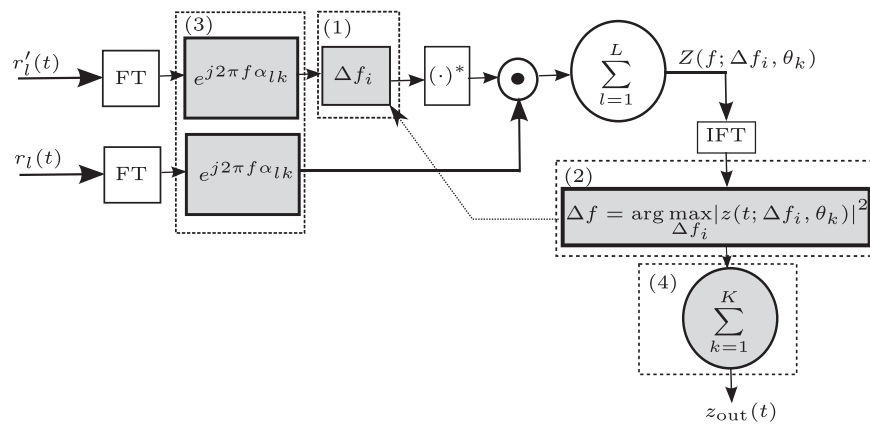
Fig. 1. Block diagram of one channel of the receiver structure: Passive time-reversal (nonshaded blocks), frequency-shift passive time-reversal [non-shaded blocks plus blocks (1) and (2)] and beamformer frequency-shift passive time-reversal receiver (all blocks).

2.1 The passive time reversal (pTR)

The basic pTR receiver is obtained from the block diagram of Fig. 1 by following the path without the gray-shaded blocks and allows obtaining the following array output (in the frequency domain):

$$Z(f) = \sum_{p=1}^{P} h_p h'^*_p S(f - \nu_p) S^*(f - \nu'_p) e^{-j2\pi f(\tau_p - \tau'_p)} e^{j2\pi(\nu_p \tau_p - \nu'_p \tau'_p)}, \tag{3}$$

where it was assumed that the cross-sensor array summation was sufficient to eliminate the cross path terms. Without loss of generality, the same signal $s(t)$ was used as probe and as message bearing signal. In actual communications, the probe signal will be the signaling pulse shape, while $s(t)$ will carry the information sequence $a(n)$. In case of perfect channel match, which will most likely happen only in the first few instants after probe transmission, we will have $h_p = h'_p$, $\tau_p = \tau'_p$ and $\nu_p = \nu'_p$, giving rise, from (3), to the inverse FT time response

$$z_{\text{out}}(t) = \sum_{p=1}^{P} |h_p|^2 C_s(t) e^{j2\pi\nu_p t}, \tag{4}$$

where $C_s(t)$ is the autocorrelation of signal $s(t)$.

2.2 The frequency-shift passive time reversal (FS-pTR)

The objective of this algorithm is to compensate for the Doppler effect produced by the movement of the emitting source, either in range or in range and depth. Taking into account blocks 1 and 2 of Fig. 1, the array output of FS-pTR becomes

$$Z(f;\Delta f) = \sum_{p=1}^{P} h_p h'^*_p S(f - \nu_p) S^*(f - \Delta f - \nu'_p) e^{-j2\pi[f\tau_p - (f-\Delta f)\tau'_p]} e^{j2\pi(\nu_p \tau_p - \nu'_p \tau'_p)} \sum_{l=1}^{L} e^{-j2\pi\Delta f \alpha_{lp}}, \tag{5}$$

where the "optimal" frequency shift Δf maximizes the power of the output over a range of possible frequency shifts. It can be seen from the previous expression that Δf appears as a correction term to align ν_p and ν'_p as well as τ_p to τ'_p. The last residual L-sensor summation term in Eq. (5) taken over the P-path arrivals unfortunately shadows the output signal both in the frequency and time domain.

2.3 The beam frequency-shift passive time reversal (bFS-pTR)

In the proposed method, channel compensation is taken one step further by individually frequency shift compensating Doppler effects for each array arrival path p, incoming from angle θ_p. In fact it is well known that source movement at relative speed vector v_s will project into each ray path p, a component v_p depending on the ray launch angle θ_p. Therefore the signal received along each path will be frequency shifted by an amount proportional to v_p/c.

The receiver structure is now modified including array steering delays for forming K beams into respective directions θ_k and summing over all the beams. This is performed by including blocks 3 and 4 of Fig. 1. Following the same approach as in Secs. 2.1 and 2.2, the signal output can now be written as

$$Z(f; \Delta f, \theta_k) = \sum_{p=1}^{P} h_p h'^*_p S(f - \nu_p) S^*(f - \Delta f - \nu'_p) e^{-j2\pi[f\tau_p - (f - \Delta f)\tau'_p]} e^{j2\pi(\nu_p \tau_p - \nu'_p \tau'_p)}$$

$$\times \sum_{l=1}^{L} e^{-j2\pi\Delta f(\alpha_{lp} - \alpha_{lk})}, \tag{6}$$

where $\alpha_{lk} = (l - 1)d \cos(\theta_k)/c$, is the delay applied to sensor l to steer beam k to direction θ_k. In the preceding expression, the last term is a beamformer response to incoming ray from direction θ_p when steered to θ_k. Its output will be maximum for $\theta_k = \theta_p$ and greatly reduced for all the other angles. Therefore the search of the maximum output power as a function of frequency shift will occur for each beam in blocks (1) and (2) and then summed up for all the beams in block (4) (of Fig. 1). So the difference introduced in bFS-pTR relative to FS-pTR is that Doppler compensation is now specific for each acoustic path. This compensation is achieved by matching the signal along each path with a time-reversed Doppler shifted replica of the acoustic field, so there is no need to explicitly know the number of paths or their propagation delays. Its limitations are associated with the beam space resolution achievable with a given array geometry.

3. Experimental results

3.1 Experimental scenario and initial setup

The data set shown in this section was collected during the UAB'07 experiment in the Bay of Trondheim, Norway, in 2007. During this experiment, the source was suspended by a crane from a fixed platform, 10 m from shore, at an initial depth of 4 m. Source depth was then varied between 4 and 10 m by steps of 0.5 m at predetermined intervals. The receiver was a surface suspended VLA with 16 hydrophones uniformly spaced at 4 m between 6 and 66 m depth. The communication range was approximately 1 km with a water column depth of 12 m at source location and about 120 m at array location. A more detailed description of the experiment can be found in Ijaz *et al.*[14]

Figure 2(a) shows the channel IR estimates where it can be seen that a large number of arrivals are reaching the receiver with different delays. Figure 2(b) shows the angle of arrival of different wavefronts. It can be seen that there are two strong arrivals at approximately 3° and the third and fourth arrival at approximately 0°. Also there is another strong arrival at approximately $-30°$. The angles shown in the y axis of this plot are obtained by direct data beamforming assuming a vertical line array. In case the array has some tilt within the source-receiver propagation plane, care should be taken in mapping these angles with the true geometrical directions ($+90$ surface, -90 bottom).

3.2 Channel compensation results

The transmitted signal, presented in this section, comprised a 50 chirp signal followed by a data set of 100 s. The chirp transmission was used for the channel IR estimation
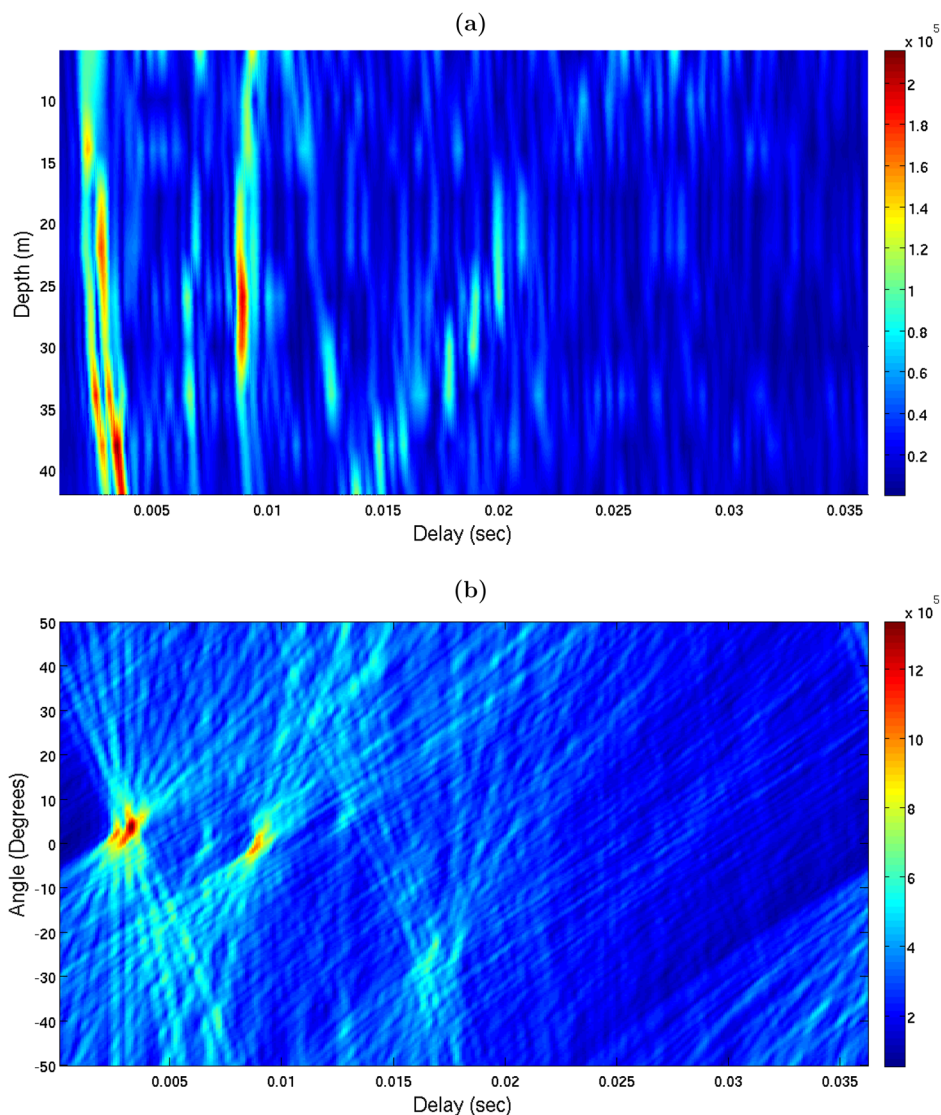
Fig. 2. (Color online) UAB'07 data set: Depth-delay channel IR estimates (a) and angle-delay plot (b), color coded in relative magnitude squared.

and to study the channel variability and Doppler spread. Each chirp has a bandwidth of 2.5 kHz ranging from 5 to 7.5 kHz with 0.1 s duration whereas data bandwidth ranges from 5.5 to 7 kHz with BPSK modulation and baud rate of 1000 bits/s. A carrier frequency of 6250 Hz was used. Figure 3(a) shows the performance of the bFS-pTR for an angular range of $-10°$ to $+10°$ compared with that of the other two algorithms, pTR and FS-pTR. During this transmission, a source depth change from 4 to 4.5 m occurred at time 12 s. It can be seen that bFS-pTR clearly outperforms both FS-pTR and pTR with a mean MSE gain of 1.8 and 2.8 dB, respectively. Figure 3(b) shows the performance in the same data set, but the angular range of the bFS-pTR is increased to $-50°$ to $+50°$, therefore including all the visible arrivals of Fig. 2 and where the improvement in performance relative to the previous case is clearly visible. The MSE performance of bFS-pTR results in a mean MSE gain of 4.9 dB. On the other hand, the performance of pTR and FSpTR degrades by 1 and 0.7 dB,
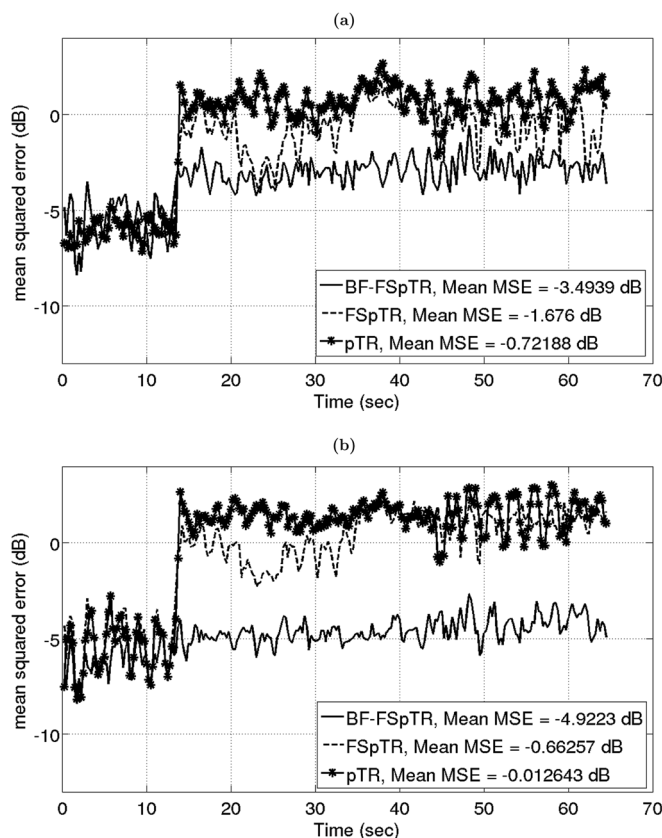
Fig. 3. UAB'07 data MSE performance comparison among pTR, FSpTR, and bFSpTR, considering an angular range of $-10°$ to $+10°$ (a) and considering an angular range of $-50°$ to $+50°$ (b).

respectively; this is due to the increase in the size of impulse response time window, increasing the number of uncompensated paths. The effect of increasing the angular range can be related to Fig. 2(b) where the inclusion of all arrivals and their compensation by the bFS-pTR improves the system performance and accounts for source depth movement.

4. Concluding remarks

This letter presents a modified passive time-reversal technique for underwater communications in presence of source depth variations during signal transmission. This technique takes advantage of the existing sensor array for compensating source depth induced Doppler variations along each path through beam separation. This is achieved by inserting the appropriate angle shifts in the pTR processor and applying frequency shifts that maximize the focused signal power output for each beam separately. This output is now focused in time and space for each arrival angle and then summed up over all beam angles for higher gain and interference rejection. It is shown with experimental data where source depth was varied during transmission that the proposed method outperforms current pTR and its variant FSpTR by MSE gains of 4.9 and 4.2 dB, respectively. Thus the proposed algorithm effectively extends the ability of current pTR-based communication schemes to account for depth variations of the transmitting nodes that is likely to occur whenever autonomous vehicles and surface suspended receiving systems are involved in routine operations at sea.

References and links

[1] M. Stojanovic, L. Freitag, and M. Johnson, "Channel-estimation-based adaptive equalization of underwater acoustic signals," in *Proceedings of the MTS/IEEE Oceans 1999*, Seattle, WA (September 1999), pp. 985–990.

[2] G. F. Edelmann, W. S. Hodgkiss, S. Kim, W. A. Kuperman, H. C. Song, and T. Akal, "Underwater acoustic communications using time-reversal," in *Proceedings of the MTS/IEEE Oceans 2001*, Honolulu, HI (November 5–8, 2001), pp. 2231–2235.

[3] D. Rouseff, "Intersymbol interference in underwater acoustic communications using time-reversal signal processing," J. Acoust. Soc. Am. **117**(2), 780–788 (2005).

[4] J. C. Preisig, "Performance analysis of adaptive equalization for coherent acoustic communications in the time-varying ocean environment," J. Acoust. Soc. Am. **118**, 263–278 (2005).

[5] T. H. Eggen, A. B. Baggeroer, and J. C. Preisig, "Communication over Doppler spread channels. II: Receiver characterization and practical results," IEEE J. Ocean. Eng. **26**(4), 612–621 (2001).

[6] A. Song, M. Badiey, H. C. Song, W. S. Hodgkiss, M. B. Porter, and KauaiEx Group, "Impact of ocean variability on coherent underwater acoustic communications during the kauai experiment (kauaiex)," J. Acoust. Soc. Am. **123**(2), 856–865 (2008).

[7] S. Ijaz, A. J. Silva, O. C. Rodriguez, and S. M. Jesus, "Doppler domain decomposition of the underwater acoustic channel response," in *Proceedings of Oceans 2011 MTS/IEEE Conference*, Santander, Spain (June 2011).

[8] L. R. LeBlanc, "Angular-spectral decomposition beamforming for acoustic arrays," IEEE J. Ocean. Eng. **9**(1), 31–39 (1984).

[9] J. P. Gomes, A. Silva, and S. M. Jesus, "Adaptive spatial combining for passive time-reversed communications," J. Acoust Soc. Am. **124**(2), 1038–1053 (2008).

[10] B. S. Sharif, J. Neasham, O. R. Hinton, and A. E. Adams, "A computationally efficient Doppler compensation system for underwater acoustic communications," IEEE J. Ocean. Eng. **25**(1), 52–61 (2000).

[11] A. Silva, S. M. Jesus, and J. P. Gomes, "Environmental equalizer for underwater communications," in *Proceedings of Oceans MTS/IEEE 2007*, Vancouver, BC, Canada (October 2007).

[12] U. Vilaipornsawai, A. Silva, and S. M. Jesus, "Underwater communications for moving source using geometry-adapted time reversal and DFE: UAN10 data," in *Proceedings of the MTS/IEEE Oceans 2011*, Santander, Spain (June 2011).

[13] F. Hlawatsch and G. Matz, *Wireless Communications over Rapidly Time-Varying Channels* (Elsevier, Burlington, VT, 2011).

[14] S. Ijaz, A. Silva, and S. M. Jesus, "Compensating for source depth change and observing surface waves using underwater communication signals," in *Proceedings of the International Conference on Sensor Technologies and Applications*, Venice, Italy (July 2010).